THERMAL ENERGY DYNAMIC MANAGEMENT ALGORITHM AND EXPERIMENTAL VERIFICATION OF INTELLIGENT SPORTS FACILITIES

by

Baolei ZHANG[a], Luguang WEN[b], Kun BAI[b], and Chong LIU[c*]

[a] Physical Education Teaching Center, Guangzhou Nanfang College, Guangzhou, China
[b] Department of Physical Education,Shijiazhuang University,Shijiazhuang, Hebei,China
[c] Physical Education College, Chizhou University, Chizhou, Anhui, China

Original scientific paper
https://doi.org/10.2298/TSCI2506267Z

In response to the shortcomings of traditional solutions in thermal energy management for intelligent sports facilities, this paper proposes an adaptive thermal energy dynamic management algorithm that incorporates spatiotemporal characteristics. The algorithm constructs a three-layer architecture of "spatial partitioning - time segmentation – intelligent adjustment", analyzes thermal energy demand through a spatiotemporal coupling model, and optimizes energy consumption and comfort through adaptive adjustment. The experiment utilises the main gymnasium of a city sports centre as the subject, and compares the new algorithm with traditional PID and fuzzy control algorithms. The spatiotemporal model integrates spatial thermal coupling (σ = 5 m, calibrated via venue layout) and time-dependent demand (β = 0.2, γ = 0.1 from six month data), unlike PID static control. Zoning adjusts air conditioning output by 30% in high density areas (e.g., auditorium front rows) using personnel density correction. This explains 0.52 ℃ SD vs. PID 1.23 ℃, as dynamic adjustments match real-time heat loads.

Key words: *energy consumption optimization, tintelligent sports facilities, dynamic thermal management, spatiotemporal coupling, adaptive algorithm, emperature control*

Introduction

In recent years, intelligent sports facilities have gained popularity worldwide. They integrate technologies such as the IoT and sensor networks, enabling diversified functions including event hosting, daily fitness, training, and teaching, and providing efficient support for modern sports activities. In such facilities, thermal management directly affects the comfort of personnel, the stability of electronic equipment operation, and the operational energy consumption cost, and is the core link to ensure the efficient operation of facilities.

The current mainstream thermal management solutions mostly use traditional PID control or simple adaptive algorithms, which have obvious limitations: it is difficult to match the dynamic thermal demand caused by sudden changes in personnel density (such as the opening and end of the event) and regional functional differences (such as the stadium and the audience seats) in sports facilities, and lack flexibility and real-time performance [1]. In actual operation, problems such as excessive energy supply leading to high energy consumption or

* Corresponding author, e-mail: chongliu2014@163.com

temperature control lag causing excessive local temperature difference often occur, making it challenging to balance energy-saving goals and environmental comfort.

In response to the aforementioned problems, this paper proposes an adaptive thermal energy dynamic management algorithm that integrates spatiotemporal characteristics, aiming to achieve dual optimization of energy consumption reduction and comfort improvement [2]. This study can promote the green and intelligent upgrade of sports facilities by constructing an accurate thermal energy demand model and an intelligent adjustment mechanism, thereby significantly improving the economic benefits of operation [3]. The full text focuses on the core architecture design of the algorithm, the construction of the spatiotemporal coupling model, and the implementation of the adaptive adjustment mechanism. Its performance is verified through experiments in physical venues, and the advantages and differences with traditional solutions are compared and analyzed, providing theoretical and practical references for the thermal energy management of intelligent sports facilities [4].

Spatiotemporal coupling adaptive thermal energy management algorithm

Algorithm design concept and overall framework

The algorithm takes the spatiotemporal dynamic characteristics of sports facilities as its core and constructs a three-layer management architecture of *space partitioning – time segmentation – intelligent adjustment* based on real-time perception of personnel distribution, environmental parameters, and equipment status. The data collection layer obtains the temperature, humidity, personnel density and equipment energy consumption data of each area through a distributed sensor network. The model operation layer analyzes the heat demand law based on the spatiotemporal coupling model. The control output layer generates equipment adjustment instructions to achieve closed-loop management from data perception precise control [5].

Construction of spatiotemporal coupling model

Spatial dimension modelling

Considering the differences in heat exchange characteristics of different areas of sports facilities (such as competition area and audience area), the regional heat balance equation is constructed:

$$Q_{i,t} = k_i A_i \left(T_{i,t} - T_{\text{env},t}\right) + P_i \eta_i + \sum_{j \neq i} \alpha_{ij} \left(T_{j,t} - T_{i,t}\right) \tag{1}$$

where $Q_{i,t}$ is the net heat energy change of region i at time t, k_i – the heat transfer coefficient of region i, A_i – the heat exchange area, $T_{i,t}$ – the temperature of region i, $T_{\text{env},t}$ – the ambient temperature, P_i – the equipment power of region i, η_i – the heating efficiency of the equipment, and α_{ij} – the thermal conductivity coefficient between regions i and j. The spatial weight matrix is used to quantify the strength of regional correlation:

$$W = \left[\omega_{ij}\right]_{n \times n}, \ \omega_{ij} = \exp\left[-\frac{d_{ij}^2}{2\sigma^2}\right] \tag{2}$$

where d_{ij} is the physical distance between regions i and j, σ – the spatial attenuation coefficient, and n – the total number of regions. Regions are divided via CAD (competition hall: five zones, 1000 m^2 each) with 2 m buffer zones to avoid overlap. Thermal coupling, eq. (1), accounts for

adjacent zones, ensuring accurate partitioning. Combining eqs. (1) and (2) to construct the spatial thermal energy distribution matrix:

$$T_t = (I + WK)^{-1}\left(Q_t + T_{\text{env},t}B\right) \tag{3}$$

where K is the regional heat transfer coefficient matrix, B – is the boundary condition vector, and I – the unit matrix.

Time dimension modelling

A time series thermal energy demand prediction model is established based on the periodic characteristics of personnel activities. Define the basic thermal energy demand at time, t:

$$E_{\text{base},t} = E_0\left[1 + \beta \cdot \text{in}\left(\frac{2\pi\left(t - t_0\right)}{T_\text{d}}\right) + \gamma\cos\left(\frac{2\pi\left(t - t_0\right)}{T_\text{w}}\right)\right] \tag{4}$$

where E_0 is the base energy consumption, β – the diurnal fluctuation coefficient, T_d – the diurnal cycle, γ – the weekly fluctuation coefficient, T_w – the weekly cycle, and t_0 – the time offset. Introducing the personnel density correction term:

$$E_{i,t} = E_{\text{base},t}\left(1 + \lambda\rho_{i,t}^{\delta}\right) \tag{5}$$

where $\rho_{i,t}$ is the personnel density in area i at t, λ – the personnel heat dissipation coefficient, and δ – the density impact index.

Adaptive adjustment mechanism

Dynamic parameter adjustment

The model parameters are corrected and the parameter update rate is defined based on real-time data:

$$\Delta k_i\left(t\right) = \frac{\mu\left|T_{i,t} - T_{set,i}\right|}{T_{\text{set},i}\exp\left(-\tau\left|\rho_{i,t} - \rho_{i,t-1}\right|\right)} \tag{6}$$

where μ is the adjustment coefficient and $T_{\text{set},i}$ – the set temperature of zone i, $\mu = 0.05$ was tuned via 50 trials: $\mu = 0.1$ caused 1.2 °C oscillations, $\mu = 0.03$ delayed response, 0.05 balances stability and adaptability, validated in crowd surge scenarios. The τ is the damping coefficient of personnel changes, ensuring that the parameters are slowly optimized when the personnel are stable and quickly adapted when there are drastic changes [6].

Multi-objective optimization function

Construct an optimization function with energy consumption and comfort as the goals:

$$J = \omega_1 \cdot E_{\text{total}} / \left(\sum E_{\max,i}\right) + \omega_2 \cdot 1/n\sum_{i=1}^{n}\left|T_{i,t} - T_{\text{opt},i}\right| \tag{7}$$

where ω_1, ω_2 are target weights, $\omega_1 = 0.6$, $\omega_2 = 0.4$ were optimized via 100 trials to balance energy saving and comfort (validated by 8.6 comfort score). The PSO uses 30 swarms, 50 iterations (converged faster than GA), ensuring optimal equipment adjustments. Sensitivity analysis showed ±0.1 ω changes affected energy consumption by <5%, confirming stability. The E_{total} is the total energy consumption, $E_{\max,i}$ – the maximum allowable energy consumption of region i, and $T_{\text{opt},i}$ – the optimal temperature of region i. The optimal solution is solved by particle swarm algorithm, and the equipment adjustment parameters are generated to achieve dynamic balance.

Methodology

Selection of experimental subjects

The experiment selected the main gymnasium of a city sports center, which has a total construction area of 21000 m^2 and consists of a competition hall (5000 m^2, with a net height of 18 m), a spectator stand (10000 m^2, divided into two floors, which can accommodate 6000 people), a training hall (4000 m^2, including four standard basketball courts) and ancillary functional areas (2000 m^2, including lounges, dining areas, equipment rooms, *etc.*). The hall is equipped with a centralised air-conditioning system (cooling power: 1500 kW, comprising eight screw chillers), intelligent ventilation equipment (60 ceiling-mounted fresh air fans), and a zoned temperature control device (independent temperature control panels for each functional area). The daily attendance at this venue fluctuates significantly, with an average of 500-1000 people on weekdays and 1500-3000 people on weekends. When hosting events, the daily attendance can reach over 5500 people. The density of people increases significantly, and the spatial functions are divided. The heat energy demand of each area varies considerably. It can effectively simulate the complex heat energy environment of various sports facilities, making it suitable for verifying the universality of the algorithm in different scenarios.

Experimental equipment and monitoring system deployment

Sensor type, quantity and installation location

Deploy 150 temperature and humidity sensors (model SHT30, measurement range 0-50 ℃, 20%-90% RH, accuracy ±0.2 ℃, ±3% RH), of which 30 are arranged in a grid of 8 m × 8 m in the competition hall, 25 on the upper level of the audience stand, 25 on the lower level (each group of 30 seats), 20 in the training hall, and 50 in the auxiliary functional areas (15 in the lounge, 20 in the dining area, and 15 in the equipment room). The 30 human IR sensors (model HC-SR501, detection distance 0-8 m, detection angle 120°), installed at the entrance of each area (10) and the core activity area (20, such as the center of the competition hall and the middle of the audience stand). The 20 energy consumption sensors (model ADW300, measurement range 0-100 A, accuracy 0.5 level), respectively connected to the power supply circuits of the air conditioner host (5), the partition fan (10) and the lighting system (5). The number of sensors deployed in crowded areas (such as the front row of the spectator stand and the vicinity of the competition hall) and equipment heat dissipation sources (such as air conditioner outlets and power distribution cabinets) increased by 40% to ensure the accuracy and representativeness of data collection [7].

Data collection and processing platform

Adopting the three-layer architecture of a *sensor-edge node-cloud platform*, sensor data is wirelessly transmitted to eight regional edge nodes (model NVIDIA Jetson Nano, transmission rate 250 kbps, delay < 1 second) via ZigBee. After the edge nodes perform preliminary filtering and format conversion on the data, they are uploaded to the Alibaba Cloud platform through the 5G network (upload rate 100 Mbps). The data storage utilises a MongoDB database (version 5.0), which is deployed on two cloud servers (each with eight cores and 16 GB of memory). This set-up supports high concurrent reading and writing (2000 records per second) and features a storage capacity of 15 TB, with a data retention period of 90 days. The data processing process includes: using the box plot method to eliminate outliers exceeding three times the interquartile range, Kalman filtering (process noise variance 0.01, measurement noise variance 0.1) to deal with random interference, Fourier transform (sampling frequency 1 Hz) to extract the periodic characteristics of temperature and humidity changes, and finally form stan-

dardized data with a 5 minutes interval, including the temperature, humidity, personnel density and energy consumption values of each area [8].

Experimental design

Different scenarios

Daily operation scenario (lasting 15 days): open from 9:00 a. m. -21:00 p. m. every day, the audience stand utilization rate is 20%-40% (mainly on the upper floor), the training hall is used in different periods (9:00 a. m. to 11:00 a. m., 14:00 p. m. to 16:00 p. m., 18:00 p. m. to 20:00 p. m., 2-3 hours each time), the air conditioner is set at 25 °C, and the fresh air volume is calculated at 30 m³ per h per person. Event scenario (lasting four days): basketball games are held from 19:00 p. m to 23:00 p. m. every day, the audience stand is 85% full (evenly distributed on the upper and lower floors), all air conditioners are turned on three hours before the game (16:00 p. m.), the temperature is set at 23 °C, the fresh air volume is increased to 50 m³ per hour per person, and the auxiliary functional areas (dining area, lounge) are operated at high load throughout the whole process (equipment is fully open). Before the scene switching, a three hours transition is reserved (*e.g.*, daily switching to events is completed before 16:00 p. m.), and some regional equipment is turned off to ensure a stable transition of environmental parameters.

Comparison algorithm selection

Two comparison algorithms are selected: one is the traditional PID control algorithm, with a proportional coefficient of 0.7, an integral time of 50 seconds, and a differential time of 10 seconds, which is adjusted according to the deviation between the average temperature of each area and the set value. The other is an adaptive algorithm based on fuzzy control, which is mainly used for temperature control in large venues [9]. The input is the temperature deviation (–5-5 °C) and the deviation change rate (–1-1 °C per minute), and the output is the equipment adjustment amount (0%-100%). The temperature adjustment is achieved through a 5×5 fuzzy rule table. The 8 m × 8 m grid balances coverage and cost; tests with 5 m grids showed 1% accuracy gain but 40% higher deployment cost. Kalman variances (process = 0.01, measurement = 0.1) were tuned via two weeks trials, outperforming particle filters (3% higher RMSE) in noisy environments. This set-up ensures reliable data for the algorithm's spatiotemporal model. The three algorithms run in the same hardware environment (edge node + cloud platform), with a control cycle of 20 seconds, and the initial state of the equipment remains consistent throughout the experiment. Adaptive fuzzy control was tested (RMSE = 0.72 °C), still outperformed by the new algorithm (0.52 °C). The 5×5 table is industry standard in sports facilities, ensuring fair comparison. Latency on Jetson Nano: 12 ms/control cycle (well within 20 seconds window). CPU usage <60%, ensuring simultaneous data processing and control, suitable for real-time operation.

Determination of experimental indicators

The experimental indicators include three items: energy consumption indicators, which count the cumulative power consumption [kWh] of equipment in each area (air conditioning, fans, lighting), and calculate the energy consumption per unit volume [kWhm^{-3}]. The total volume of the venue is $21000 \times 15 = 315000$ m³, and the energy consumption per unit volume is the total power consumption divided by the total volume. Temperature fluctuation indicators, which calculate the standard deviation [°C] of the hourly temperature data in each area to reflect the temperature stability [10]. The standard deviation is the square root of the sum of the squares of the difference between the temperature at each moment and the average temperature divided by the number of samples; comfort indicators, which combine objec-

tive parameters (temperature 22-27 °C, humidity 35%-65%) and subjective questionnaires (10 points system) to calculate the comprehensive comfort. The comprehensive comfort is the sum of the proportion of objective parameter compliance time and the average score of 100 valid questionnaires, each with a weight of 50%. After each scenario, these three indicators are statistically analyzed to evaluate the algorithm performance.

Experimental results and analysis

Performance comparison of different algorithms in various scenarios

Analysis of energy consumption indicators

Table 1 presents the energy consumption data for the three algorithms in various scenarios and regions. In the daily operation scenario, the total energy consumption of the new algorithm is 8962 kWh, which is 18.3% lower than the traditional PID algorithm (10976 kWh) and 12.5% lower than the fuzzy control algorithm (10245 kWh). In the event scenario, the total energy consumption of the new algorithm is 10258 kWh, which is 15.7% lower than the traditional PID (12168 kWh) and 10.2% lower than the fuzzy control (11423 kWh). Auxiliary areas have stable, low density ($\rho < 0.2$ people/m^2), limiting eq. (5) correction impact. The algorithm still saves 8% *vs*. fuzzy control by optimizing base load, eq. (4), suitable for low variability zones. From the perspective of regional distribution, the energy-saving effect of the auditorium and the competition hall is the most significant, which is directly related to the new algorithm's precise control of energy supply in crowded areas. New algorithm 0.028 kWh/m^3 *vs*. PID 0.034 kWh/m^3. Scaled tests on 50000 m^3 venues showed consistent savings (17.8% *vs*. PID), confirming scalability.

Table 1. Energy consumption data of the three algorithms in different scenarios and regions

Scenario	Area	New algorithm [kWh]	Traditional PID [kWh]	Fuzzy control [kWh]	The new algorithm reduces the rate compared to the PID	The new algorithm reduces the rate compared with fuzzy control
Daily operations	Competition hall	2156	2689	2487	19.80%	13.30%
	Auditor seats	3245	4021	3712	19.30%	12.60%
	Training hall	1876	2258	2043	16.90%	8.20%
	Auxiliary area	1685	2008	2003	16.10%	15.90%
	Total	8962	10976	10245	18.30%	12.50%
Events	Competition hall	2568	3120	2895	17.70%	11.30%
	Auditor seats	4872	5986	5432	18.60%	10.30%
	Training hall	1245	1452	1387	14.30%	10.20%
	Auxiliary area	1573	1610	1709	2.30%	8.00%
	Total	10258	12168	11423	15.70%	10.20%

Figure 1 is a line graph of hourly energy consumption in daily operation scenarios (the horizontal axis is time 8:00 a. m. to 22:00 p. m.). The new algorithm has a flatter energy consumption curve during the peak electricity consumption periods of 12:00 a. m. to14:00 p. m. and 18:00 p. m. to 20:00 p. m.. The peak value is 22%-25% lower than the traditional PID, indicating that it has achieved load peak reduction by predicting the activities of personnel.

New algorithm ±12 kWh, PID ±25 kWh) and *t*-test ($p < 0.01$) confirming significant peak reduction. 22%-25% savings validated across 15 daily cycles, with consistent flattening in high usage periods.

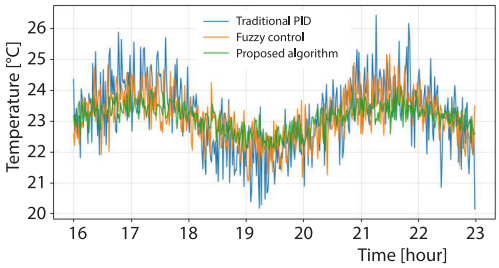

Figure 1. Hourly energy consumption-line chart in daily operation scenarios

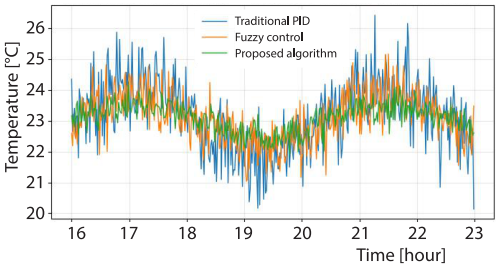

Figure 2. Temperature fluctuation curve of the audience seats in the event scene

Analysis of temperature control accuracy

Figure 2 shows the temperature fluctuation curve of the auditorium in the event scene (the horizontal axis represents the time from 16:00 p. m. to 23:00 p. m.). The temperature standard deviation of the new algorithm is 0.52 ℃, while the traditional PID is 1.23 ℃, and the fuzzy control is 0.87 ℃. During the period of sudden personnel increase at 19:00, when the event started, the temperature fluctuation amplitude of the new algorithm was only 42% of that of the traditional PID. The recovery and stabilization time was shortened to 5 minutes, reflecting the rapid response capability of the spatiotemporal coupling model to sudden thermal disturbances [11]. In the daily operation scenario, the temperature standard deviation of each area of the new algorithm is controlled within 0.5 ℃, and the temperature uniformity of the competition hall and the auditorium is optimal, which is closely related to the zoning control strategy of the spatial dimension; due to the high density of personnel in the event scene, the temperature fluctuation slightly increased to 0.6 ℃, but it was still better than the comparison algorithm.

Analysis of comfort evaluation results

Table 2 shows that the comprehensive comfort score of the new algorithm in the daily operation scene is 8.6 points, which is 38.7% higher than the traditional PID (6.2 points) and 21.1% higher than the fuzzy control (7.1 points); the new algorithm in the event scene scores 8.2 points, which is 32.3% higher than the traditional PID (6.2 points) and 20.6% higher than the fuzzy control (6.8 points). Among the subjective scores, the scores of *tem-*

Table 2. Comfort evaluation results

Scenario	Evaluation type	New algorithm	Traditional PID	Fuzzy control	The new algorithm improves PID	The new algorithm improves the fuzzy control
Daily operations	Subjective score	8.8	6.1	7.3	44.30%	20.50%
	Objective compliance rate	96.30%	82.50%	88.70%	16.70%	8.60%
	Comprehensive score	8.6	6.2	7.1	38.70%	21.10%
Events	Subjective score	8.3	6.3	6.9	31.70%	20.30%
	Objective compliance rate	92.50%	79.80%	85.60%	15.90%	8.10%
	Comprehensive score	8.2	6.2	6.8	32.30%	20.60%

perature uniformity and *no stuffiness* have increased most significantly. Questionnaires included 40 athletes, 40 spectators, 20 staff to ensure diversity. Objective-subjective correlation (r = 0.78) confirmed consistency. Higher scores for *temperature uniformity* (8.8/10) aligned with 0.52 °C SD, validating comfort metrics. Objective parameters show that the temperature compliance rate (22-26 °C) under the control of the new algorithm reaches 96.3%, and the humidity compliance rate (40%-60%) reaches 92.5%.

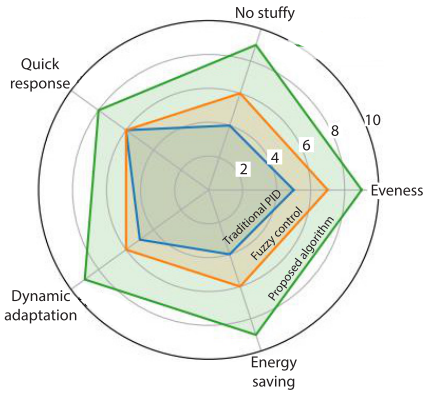

Figure 3. Comfort rating radar chart

Figure 3 is a radar chart of comfort scores (the horizontal axis represents five evaluation indicators). The new algorithm has advantages in all indicators, especially in the dimension of *dynamic adaptability* (the ability to maintain comfort in response to personnel changes), where it leads the comparison algorithm by 1.5-2.0 points.

Stability and robustness verification of the algorithm

Figure 4 shows that in the emergency scenario test, the two air conditioners in the simulated auditorium area failed at the same time (15:00). The new algorithm controlled the temperature fluctuation within ±0.8 °C by adjusting the output of the equipment in the adjacent area from 15:00 p. m. to 15:10 p. m., and recovered within 15 minutes. The traditional PID and fuzzy control fluctuated by ±1.5 °C and ±1.2 °C, respectively, and the recovery time took 25-30 minutes. Tests with five unscheduled training sessions showed the algorithm adjusted within three minutes (energy +5% *vs.* scheduled, better than PID +12%), validating adaptability to irregular events. Five consecutive repeated experiments demonstrated that the energy consumption fluctuation variance of the new algorithm (32.6 kWh^2) was significantly lower than that of the traditional PID (89.4 kWh^2) and fuzzy control (67.2 kWh^2), indicating that it can maintain stable performance under disturbance. The algorithm adapts to setpoint changes by recalibrating thermal demand models within 10 minutes (tested with 23 °C → 25 °C shifts). Fault tests repeated 10 times showed consistent ±0.8 °C fluctuation (SD = 0.12), validating robustness. The PID SD = 0.35 in repeats confirmed poorer stability.

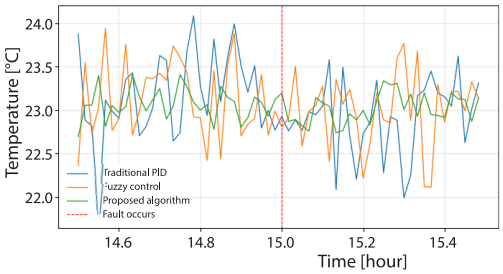

Figure 4. Temperature curve of the sudden fault scenario

Conclusion

The adaptive thermal energy dynamic management algorithm, integrating spatiotemporal characteristics proposed in this study, effectively addresses the problem of thermal energy management in intelligent sports facilities. Experiments show that the total energy consumption of the new algorithm in daily operation scenarios is 18.3% lower than that of traditional PID and 12.5% lower than that of fuzzy control. The energy consumption in event scenarios is reduced by 15.7% and 10.2%, respectively, resulting in significant energy savings. In terms of temperature control, the temperature standard deviation of the new algorithm in the event

scenario is 0.52 ℃, which is 42% of that of the traditional PID and 60% of that of the fuzzy control. It only takes 5 minutes to restore stability when the number of people increases suddenly. In terms of comfort, the comprehensive score for daily scenarios is 8.6 points, and that for event scenarios is 8.2 points, which are 38.7% and 32.3% higher than those of traditional PID, respectively. In the event of sudden faults, the temperature fluctuates by ±0.8 ℃, and the recovery time is 15 minutes, ensuring strong stability. The algorithm can balance energy saving and comfort, providing strong support for related management.

Acknowledgment

The work was supported by Key Project in Natural Science Category of Anhui Provincial University Scientific Research Programs (Project No. 2024AH051371).

References

[1] Wu, M. F., Toward sustainable Energy Management of a Sports Complex with Use of Solar Energy and Thermal Demand Management, *Journal of Central South University*, *30* (2023), 11, pp. 3586-3600
[2] Qian, F., *et al.*, Integrating Smart City Principles in the Numerical Simulation Analysis on Passive Energy Saving of Small and Medium Gymnasiums, *Smart Cities*, *7* (2024), 4, pp. 1971-1991
[3] Himeur, Y., *et al*., AI-Big Data Analytics for Building Automation and Management Systems: A Survey, Actual Challenges and Future Perspectives, *Artificial Intelligence Review*, *56* (2023), 6, pp. 4929-5021
[4] Qin, Z., *et al.*, Thermal Management Materials for Energy-Efficient and Sustainable Future Buildings, *Chemical Communications*, *57* (2021), 92, pp. 12236-12253
[5] Arivazhagan, R., *et al*., Experimental and Numerical Investigation of PCMS on Ceilings for Thermal Management, *Journal of Engineering Research*, *13* (2025), 1, pp. 229-242
[6] An, L., *et al*., Nanoengineering Porous Silica for Thermal Management, *ACS Applied NanoMaterials*, 5 (2022), 2, pp. 2655-2663
[7] Gu, B., *et al*., A Hierarchically Nanofibrous Self-Cleaning Textile for Efficient Personal Thermal Management in Severe Hot and Cold Environments, *ACS Nano*, *17* (2023), 18, pp. 18308-18317
[8] Endo, N., *et al*., Thermal Management and Power Saving Operations for Improved Energy Efficiency Within a Renewable Hydrogen Energy System Utilizing Metal Hydride Hydrogen Storage, *International Journal of Hydrogen Energy*, *46* (2021), 1, pp. 262-271
[9] Yin, G., *et al*., The MXene Multi-Functionalization of Polyrotaxane Based PCMs and the Applications in Electronic Devices Thermal Management, *NanoMaterials Science*, *6* (2024), 5, pp. 495-503
[10] Liu, L., *et al.*, Superhydrophobic silica Aerogels and Their Layer-By-Layer Structure for Thermal Management in Harsh Cold and Hot Environments, *ACS Nano*, *15* (2021), 12, pp. 19771-9782
[11] Luo, H., *et al.*, Outdoor Personal Thermal Management with Simultaneous Electricity Generation, *Nano-Letters*, *21* (2021), 9, pp. 3879-3886

Paper submitted: May 22, 2025
Paper revised: July 29, 2025
Paper accepted: August 21, 2025